


Memory effects for a stochastic fractional oscillator in a magnetic field

Romi Mankin, Katrin Laas, Tõnu Laas,* and Sander Paekivi

School of Natural Sciences and Health, Tallinn University, 29 Narva Road, 10120 Tallinn, Estonia (Received 31 August 2017; revised manuscript received 24 December 2017; published 26 January 2018)

The problem of random motion of harmonically trapped charged particles in a constant external magnetic field is studied. A generalized three-dimensional Langevin equation with a power-law memory kernel is used to model the interaction of Brownian particles with the complex structure of viscoelastic media (e.g., dusty plasmas). The influence of a fluctuating environment is modeled by an additive fractional Gaussian noise. In the long-time limit the exact expressions of the first-order and second-order moments of the fluctuating position for the Brownian particle subjected to an external periodic force in the plane perpendicular to the magnetic field have been calculated. Also, the particle's angular momentum is found. It is shown that an interplay of external periodic forcing, memory, and colored noise can generate a variety of cooperation effects, such as memory-induced sign reversals of the angular momentum, multiresonance versus Larmor frequency, and memory-induced particle confinement in the absence of an external trapping field. Particularly in the case without external trapping, if the memory exponent is lower than a critical value, we find a resonancelike behavior of the anisotropy in the particle position distribution versus the driving frequency, implying that it can be efficiently excited by an oscillating electric field. Similarities and differences between the behaviors of the models with internal and external noises are also discussed.

DOI: [10.1103/PhysRevE.97.012145](https://doi.org/10.1103/PhysRevE.97.012145)**I. INTRODUCTION**

The harmonic oscillator is the simplest toy model for different phenomena in nature and as such it is a typical theoretician's paradigm for various fundamental conceptions [1]. Since Chandrasekhar [2] originally considered the problem of noise-driven dynamics of a Brownian harmonic oscillator, noisy oscillators have been a subject extensively investigated in different fields including physics [3,4], biology [5], and chemistry [6]. In most of the previous analysis the influence of white as well as colored noises on oscillators characterized by Stokes friction dynamics have been considered [7]. Particularly, it is shown that the influence of colored noise on the oscillator frequency may lead to different resonant phenomena. First, it may cause energetic instability, which manifests itself in an unlimited increase of the second-order moments of the output with time, while the mean value of the oscillator displacement remains finite [8–10]. Second, if the oscillator is subjected to an external periodic force and the fluctuations of the oscillator frequency are colored, the behavior of the amplitude of the first moments shows a nonmonotonic dependence on noise parameters, i.e., stochastic resonance [11–13]. Third, in some cases a bona fide resonance appears, where the moments and the signal-to-noise ratio show a nonmonotonic dependence on the frequency of external forcing [10,14].

A popular generalization of the harmonic oscillator consists in replacing the usual Stokes friction term in the dynamical equation for a harmonic oscillator by a generalized friction term with a power-law memory [15–21]. The dynamical equation for such an oscillator is a special case of the more general fractional Langevin equation (see, e.g., [22]). The

main advantage of this equation is that it provides a physically transparent and mathematically tractable description of the stochastic dynamics in systems with slow relaxation processes and with anomalous slow diffusion (subdiffusion). Notably, experiments from many different areas reveal that anomalous diffusion with a mean-square displacement of particles $\langle r^2(t) \rangle \sim t^\alpha$, ($\alpha \neq 1$) is ubiquitous in nature, signaling that slow transport, $\alpha < 1$, may be generic for complex heterogeneous materials [23]. Examples of such systems are supercooled liquids, glasses, colloidal suspensions, polymer solutions [24,25], viscoelastic media, amorphous semiconductors [26–28], the cytoplasm of living cells [29], and large proteins [30]. This method has also been successfully used in describing anomalous diffusion phenomena for nuclear fusion reactions [31] and for the interpretation of experimental data for dusty plasmas [32–35].

Diffusion of particles in plasmas exposed to an external magnetic field still remains one of the important problems of plasma physics and controlled fusion [36]. In this context, the stochastic dynamics of charged Brownian particles as well as an ordinary harmonic oscillator embedded in a magnetic field driven by internal or external noises has been a topic of great interest, widely studied in the literature [2,3,36–38]. It is important to notice that although the behavior of the stochastic diffusion process of a charged classical harmonic oscillator in a constant magnetic field has been theoretically investigated in detail (see, e.g., Refs. [3,37]), it seems that proper analysis of the potential consequences of an interplay of colored noise, external periodic forcing, and memory effects in a fractional oscillator embedded in a magnetic field is still missing in literature. This is quite surprising in view of the fact that the importance of colored fluctuations and a power-law-type memory (friction with a long-time memory) for dusty plasma liquids has been well recognized [32–35,39].

*tonu.laas@tlu.ee

Motivated by the above reasons and the results of Refs. [3,20], the present paper considers a model similar to the one presented in Ref. [3], except that the Stokes-type friction term is replaced with a power-law memory kernel and that the influence of the fluctuating environment is modeled not by an additive Gaussian white noise but by an additive Gaussian fractional noise. Moreover, to make the model more general we add an external periodic force (e.g., an electric field). Thus we consider the stochastic dynamics of a charged fractional oscillator under the action of crossed periodic electric field and a constant magnetic field.

The main contribution of this paper is as follows. In the long-time limit ($t \rightarrow \infty$), we provide exact formulas for the analytical treatment of the dependence of the first- and second-order statistical moments of the fluctuating particle position and the mean angular momentum of the rotational part of particle motion in the plane perpendicular to the magnetic field on system parameters, such as the magnetic induction, the memory exponent, the intensity of the noise, the friction coefficient, and the oscillation frequency of the external periodic force. Based on those exact expressions we demonstrate that sign reversals are manifested in the dependence of the particle's mean angular momentum upon the memory exponent α as well as upon Larmor frequency and the frequency of the external drive. Furthermore, we show that in certain parameter regions the angular momentum exhibits a multiresonance behavior versus the driving frequency, and even versus Larmor frequency. As one of our main results, we establish, in the case of high values of Larmor frequency, a memory-induced strong resonancelike suppression of particles spatial dispersion at intermediate values of the memory exponent. Moreover, in the case of external fractional noise we have found a critical memory exponent α_c , which marks the transition between different dynamical regimes of the oscillator. Namely, for $\alpha < \alpha_c$, the phenomenon of memory-induced trapping occurs, i.e., at sufficiently small values of the memory exponent a bounded (in time) regime of the particle's dynamics due to the cage effect [15,21] is possible even if the trapping potential well in the dynamical equation is absent. For $\alpha > \alpha_c$ and also if the additive noise is internal, such self-trapping of a particle is impossible and particle dynamics is subdiffusive. Particularly, in the case of memory-induced trapping we find a resonancelike behavior of the anisotropy in the particle position distribution versus the driving frequency, implying that it can be efficiently excited by an oscillating external force.

The structure of the paper is as follows. In Sec. II we present the model investigated. Exact formulas are found for the analysis of the behavior of the first- and second-order moments and of the mean angular momentum. In Sec. III we analyze the dependence of the particle distribution characteristics on system parameters. Section IV contains some brief concluding remarks. Some formulas are delegated to the Appendices.

II. MODEL AND THE EXACT MOMENTS

A. Model

Consider the combined inertial and diffusive motion of a charged Brownian particle embedded in a complex viscoelastic media with memory (e.g., a dusty plasma) under the action of a

constant magnetic field and some time-dependent force fields. As a model for such a system with memory, strongly coupled with a noisy environment, we consider a generalized Langevin equation (GLE) with a harmonic confinement potential $U(\mathbf{r})$:

$$\begin{aligned} \ddot{\mathbf{r}}(t) + \frac{\tilde{\gamma}}{m} \int_0^t \eta(t-t') \dot{\mathbf{r}}(t') dt' + \frac{1}{m} \nabla U(\mathbf{r}) - \frac{q}{mc} \dot{\mathbf{r}}(t) \times \mathbf{B} \\ = \boldsymbol{\xi}(t) + \mathbf{A}_0 \cos \omega t, \end{aligned} \quad (1)$$

where $\mathbf{r} = (X, Y, Z)$ denotes the particle's position, $\dot{\mathbf{r}} \equiv d\mathbf{r}/dt$, $\eta(t)$ is the dissipative memory kernel that characterizes the viscoelastic properties of the medium, $\gamma = \tilde{\gamma}/m$ is the damping coefficient (friction coefficient), ∇ denotes the gradient operator, q is the charge of the particle with mass m , and $\mathbf{B} = (0, 0, B)$ is the intensity of the magnetic field. The external periodic force $\mathbf{A}_0 \cos \omega(t)$ per unit mass is assumed, for simplicity, to be pointing along the x axis, that is, $\mathbf{A}_0 = (A_0, 0, 0)$, and the three-dimensional trapping potential $U(\mathbf{r})$ with its minimum at $\mathbf{r}_0 = 0$ is given by

$$\frac{1}{m} U(\mathbf{r}) = \frac{\omega_0^2}{2} \mathbf{r}^2, \quad (2)$$

where ω_0 is the trap frequency. Depending on the physical situation, the zero-centered driving noise per unit mass $\boldsymbol{\xi} = [\xi_1(t), \xi_2(t), \xi_3(t)]$ can be regarded either as an internal noise, in which case its stationary correlation function satisfies Kubo's second fluctuation dissipation theorem [40] expressed as

$$\langle \xi_i(t) \xi_j(t') \rangle = k_B T \gamma \delta_{ij} \eta(|t-t'|), \quad (3)$$

where δ_{ij} denotes the Kronecker symbol, k_B is the Boltzmann constant, and T is the absolute temperature of the heat bath, or an external noise, in which case the driving noise $\boldsymbol{\xi}(t)$ and the dissipation may have different origins and no fluctuation-dissipation relation holds, i.e., $\boldsymbol{\xi}(t)$ is not related to the memory kernel $\eta(t)$. Hence, in this paper the random force $\boldsymbol{\xi}(t)$ is assumed to be the sum of two uncorrelated contributions

$$\boldsymbol{\xi}(t) = \boldsymbol{\xi}^{(1)}(t) + \boldsymbol{\xi}^{(2)}(t), \quad \langle \boldsymbol{\xi}^{(1)}(t) \boldsymbol{\xi}^{(2)}(t') \rangle = 0, \quad (4)$$

where $\boldsymbol{\xi}^{(1)}(t)$ is the internal noise due to thermal activity and $\boldsymbol{\xi}^{(2)}(t)$ is an external stationary fractional Gaussian noise with the correlation functions given by

$$\begin{aligned} C_{ij}^{(2)}(\tau) = \langle \xi_i^{(2)}(t+\tau) \xi_j^{(2)}(t) \rangle = \delta_{ij} \frac{D}{\Gamma(1-\delta)|\tau|^\delta}, \\ \langle \boldsymbol{\xi}^{(2)}(t) \rangle = 0, \end{aligned} \quad (5)$$

where $0 < \delta < 1$, D characterizes the noise intensity, and $\Gamma(\cdot)$ is the Γ function. To mimic the viscoelastic properties of the medium, the dissipative kernel $\eta(t)$ is supposed to be a power-law memory [15–17,22]:

$$\eta(t) = \frac{1}{\Gamma(1-\alpha)|t|^\alpha}, \quad (6)$$

with a memory exponent $0 < \alpha < 1$. The internal noise $\boldsymbol{\xi}^{(1)}(t)$ is assumed to be a Gaussian noise with the correlation function determined by Eqs. (3) and (6). By taking the limit $\alpha \rightarrow 1$ in Eq. (6) it follows that $\eta(t)$ possesses the properties of the δ function (its δ -functional behavior manifests itself in the integrals), and thus $\eta(t)$ at $\alpha \rightarrow 1$ corresponds to nonretarded friction (Stokes friction) in the GLE (1). It should be pointed

out that this is in fact a singular limit which must be handled with a special regularization (see, e.g., Ref. [41]). In the case of Stokes friction ($\alpha = 1$) and $\xi^{(2)}(t) = 0$, $A_0 = 0$, i.e., the external periodic drive is absent, the model (1) reduces to the model for the harmonically trapped Brownian particle in the magnetic field previously considered in Ref. [3].

Due to the linearity of the restoring force, $-\nabla U(\mathbf{r})$, the z component in Eq. (1) decouples, and the process $Z(t)$ behaves as a one-dimensional fractional oscillator considered in Refs. [15, 18, 42]. Therefore, in the rest of this paper we will consider the motion in the xy plane. In the xy plane the GLE (1) can be written as a system of dynamical equations for two coupled fractional oscillators:

$$\ddot{X} + \gamma \frac{d^\alpha}{dt^\alpha} X(t) + \omega_0^2 X(t) - \Omega \dot{Y}(t) = A_0 \cos(\omega t) + \xi_1(t), \quad (7)$$

$$\ddot{Y}(t) + \gamma \frac{d^\alpha}{dt^\alpha} Y(t) + \omega_0^2 Y(t) + \Omega \dot{X}(t) = \xi_2(t), \quad (8)$$

where $\Omega = qB/mc$ is Larmor frequency and the operator d^α/dt^α with $0 < \alpha < 1$ denotes the fractional derivative in Caputo's sense given by [43]

$$\frac{d^\alpha}{dt^\alpha} f(t) = \frac{1}{\Gamma(1-\alpha)} \int_0^t \frac{f'(t')}{(t-t')^\alpha} dt'. \quad (9)$$

Note that in the case without the magnetic field \mathbf{B} the counterparts of the model (1) with Eqs. (5) and (6) are widely used in fitting experimental data from intracellular microrheology and from single-molecule experiments probing conformational fluctuations in proteins [17, 44, 45].

B. First moments

After averaging Eqs. (7) and (8) over the ensemble of realizations of the random processes $\xi_1(t)$ and $\xi_2(t)$ we obtain

$$\frac{d^2}{dt^2} \langle X(t) \rangle + \gamma \frac{d^\alpha}{dt^\alpha} \langle X(t) \rangle + \omega_0^2 \langle X(t) \rangle - \Omega \langle \dot{Y}(t) \rangle = A_0 \cos(\omega t), \quad (10)$$

$$\frac{d^2}{dt^2} \langle Y(t) \rangle + \gamma \frac{d^\alpha}{dt^\alpha} \langle Y(t) \rangle + \omega_0^2 \langle Y(t) \rangle + \Omega \langle \dot{X}(t) \rangle = 0. \quad (11)$$

Thus it turns out that the fluctuating force $\xi(t)$ in Eq. (1) does not affect the first moments $\langle X(t) \rangle$ and $\langle Y(t) \rangle$ of the output of the fractional oscillators (7) and (8) and $\langle \mathbf{r}(t) \rangle$ remains equal to the noise-free solution. From Eqs. (10) and (11) one can easily obtain an exact linear system of four first-order integrodifferential equations for four variables: $x_1 \equiv \langle X \rangle$, $x_2 \equiv \langle \dot{X} \rangle$, $x_3 \equiv \langle Y \rangle$, and $x_4 \equiv \langle \dot{Y} \rangle$. By applying the Laplace transformation technique to these equations the solution of Eqs. (10) and (11) can be represented in the form

$$x_i(t) = \sum_{k=1}^4 H_{ik}(t) x_k(0) + A_0 \int_0^t H_{i2}(t-t') \cos(\omega t') dt', \quad (12)$$

$i = 1, \dots, 4,$

where the constants of integration $x_k(0)$ are determined by the initial conditions and the relaxation functions $H_{ik}(t)$ with $H_{ik}(0) = \delta_{ik}$ are the Laplace inversions of the Laplace transforms

$$\hat{H}_{ik}(s) = \int_0^\infty e^{-st} H_{ik}(t) dt \quad (13)$$

given by Eqs. (A2)–(A7) in Appendix A. Particularly, integral representations of the relaxation functions $H_{12}(t)$ and $H_{32}(t)$ are given by Eqs. (A8)–(A12). For large t the functions $H_{ik}(t)$ decay as a power law [see Eqs. (A13)–(A15)] and thus in the long-time limit, $t \rightarrow \infty$, the memory about the initial conditions will vanish as

$$\sum_{k=1}^4 H_{ik}(t) x_k(0) \approx \frac{\gamma x_i(0)}{\omega_0^2 \Gamma(1-\alpha) t^\alpha} + O(t^{-(1+\alpha)}), \quad i = 1, 3, \quad (14)$$

and the average particle displacement relaxes to

$$\langle X \rangle_{as} \equiv \langle X \rangle_{|t \rightarrow \infty} = A_0 |\hat{H}_{12}(-i\omega)| \cos(\omega t + \varphi_1), \quad (15)$$

$$\langle Y \rangle_{as} \equiv \langle Y \rangle_{|t \rightarrow \infty} = A_0 |\hat{H}_{32}(-i\omega)| \cos(\omega t + \varphi_3), \quad (16)$$

where the phase shifts φ_1 and φ_3 can be represented as

$$\tan \varphi_k = -\frac{\text{Im}[\hat{H}_{k2}(-i\omega)]}{\text{Re}[\hat{H}_{k2}(-i\omega)]}, \quad k = 1, 3. \quad (17)$$

So, in the long-time limit, $t \rightarrow \infty$, the mean trajectory of the particle positions is characterized by an ellipse around the minimum of the trapping potential ($\mathbf{r}_0 = 0$).

If the trapping potential is absent, $\omega_0 = 0$, the asymptotic behavior of the relaxation functions $H_{ik}(t)$ is different from the general case considered above [see also Eqs. (A16)–(A18)] and the memory about the initial conditions will not vanish. In this case the center of the characteristic ellipse, which describes the average particle trajectory at $t \rightarrow \infty$, is the initial position $(x(0), y(0))$ of the particle, i.e.,

$$\langle X \rangle_{as} = x(0) + A_0 |\hat{H}_{12}(-i\omega)| \cos(\omega t + \varphi_1), \quad (18)$$

$$\langle Y \rangle_{as} = y(0) + A_0 |\hat{H}_{32}(-i\omega)| \cos(\omega t + \varphi_3). \quad (19)$$

C. Second moments

By applying the Laplace transformation to Eqs. (7) and (8) one can easily obtain formal expressions for the displacements $X(t)$ and $Y(t)$ in the following forms:

$$X(t) = \langle X(t) \rangle + \int_0^t [H_{12}(t-t') \xi_1(t') - H_{32}(t-t') \xi_2(t')] dt', \quad (20)$$

$$Y(t) = \langle Y(t) \rangle + \int_0^t [H_{32}(t-t') \xi_1(t') + H_{12}(t-t') \xi_2(t')] dt', \quad (21)$$

where the averages $\langle X(t) \rangle$ and $\langle Y(t) \rangle$ are given by Eq. (12).

In the following, our interest is focused on the long-time regime, $t \rightarrow \infty$, where the harmonically trapped

particle ($\omega_0 \neq 0$) has lost all memory of the initial conditions. We consider the second moments $\sigma_{xx} \equiv \langle [X(t) - \langle X(t) \rangle]^2 \rangle$, $\sigma_{yy} \equiv \langle [Y(t) - \langle Y(t) \rangle]^2 \rangle$, $\sigma_{xy} \equiv \langle [X(t) - \langle X(t) \rangle][Y(t) - \langle Y(t) \rangle] \rangle$, which determine the particle's positional distribution function. Since the magnetic field leads to the rotation of charged particles in the xy plane we also consider the mean angular momentum of the particles $\langle L_z(t) \rangle = \langle X(t)\dot{Y}(t) - Y(t)\dot{X}(t) \rangle$.

Using Eqs. (20), (21), and (5) we obtain

$$\sigma_{xy}(t) = 0 \quad (22)$$

and

$$\sigma_{xx}(t) = \sigma_{yy}(t) = 2 \int_0^t [H_{12}(t_1)M_1(t_1) + H_{32}(t_1)M_3(t_1)]dt_1, \quad (23)$$

where the involved functions M_1 and M_3 are given by [see Eqs. (3) and (5)]

$$M_k(t) = \int_0^t C_{kk}(t-t_1)H_{k2}(t_1)dt_1, \quad k = 1, 3, \quad (24)$$

and

$$C_{kk}(t) = C_{kk}^{(2)}(t) + k_B T \gamma \eta(t). \quad (25)$$

To discern the effects caused by additive external and internal noises in the behavior of the second moments $\sigma_{xx}(t)$ and $\langle L_z(t) \rangle$, we will henceforth consider the cases of external noise and internal noise separately. Moreover, as the model (1) driven by an internal noise $\xi(t) = \xi^{(1)}(t)$ can be considered as a particular case of the model driven by an external noise $\xi(t) = \xi^{(2)}(t)$ with $\delta = \alpha$ and $D = k_B T \gamma$, we will mainly restrict our following analysis to the case of external noise. In the general case $\xi(t) = \xi^{(1)}(t) + \xi^{(2)}(t)$ the second moments $\sigma_{xx}(t)$ and $\langle L_z(t) \rangle$ can be found as the summation of the contributions generated by $\xi^{(1)}(t)$ and $\xi^{(2)}(t)$, separately.

In the long-time limit, another representation of $\sigma_{xx}(t)$, which is more convenient for numerical calculations and for analysis of the dependence on system parameters, is given by Eqs. (B1) and (B2) in Appendix B. In the case of a free particle, i.e., $\omega_0 = 0$, the asymptotic behavior of the variance $\sigma_{xx}(t)$ depends strongly on the values of the memory exponent α and of the noise exponent δ . From Laplace transforms of $M_k(t)$,

$$\hat{M}_k(s) = Ds^{\delta-1} \hat{H}_{k2}(s), \quad k = 1, 3, \quad (26)$$

and Eqs. (A2) and (A3) it follows that in the long-time limit

$$M_1(t) \sim \frac{D}{\gamma \Gamma(1-\delta+\alpha)} \times \frac{1}{t^{\delta-\alpha}},$$

$$M_3(t) \sim -\frac{D\Omega}{\gamma^2 \Gamma(2\alpha-\delta)} \times \frac{1}{t^{1+\delta-2\alpha}}. \quad (27)$$

Now, taking into account Eqs. (A17) and (A18), one can use Eq. (27) to obtain that the integral (23) converges to a finite value only if

$$2\alpha < \delta < 1. \quad (28)$$

Thus, if the inequalities (28) are valid, the phenomenon of memory-induced trapping occurs [15,21]; in the opposite case the dynamics of the Brownian particle is either subdiffusive as

for $2\alpha > \delta > 2\alpha - 1$ or superdiffusive if $\delta < 2\alpha - 1$, $\alpha > \frac{1}{2}$ with

$$\sigma_{xx}(t) = \sigma_{yy}(t) \simeq \frac{2D}{\gamma^2(2\alpha-\delta)\Gamma(\alpha)\Gamma(1+\alpha-\delta)} t^{2\alpha-\delta},$$

$$t \rightarrow \infty. \quad (29)$$

In the case of Stokes friction ($\alpha = 1$) the asymptotic behavior of the variance $\sigma_{xx}(t)$ must be handled with care. The direct inserting $\delta = \alpha = 1$ into Eq. (29) yields $\sigma_{xx}(t) \simeq 2k_B T t / \gamma$, which is independent of the Larmor frequency Ω , but the correct result reads [46]

$$\sigma_{xx}(t) \simeq \frac{2k_B T \gamma t}{\gamma^2 + \Omega^2}, \quad \alpha = \delta = 1, \quad t \rightarrow \infty. \quad (30)$$

In Appendix C we consider some peculiarities of the case of an internal noise. Particularly, it is pointed out that by $\alpha = 1$ the relaxation functions decay exponentially, i.e., a slow relaxation of power-law order is absent [see also Eq. (C4)]. In this case the power-law asymptotic formula (29) is not applicable. Thus the model (1) driven by an internal noise without external trapping, $\omega_0 = 0$, predicts in the asymptotic regime ($t \rightarrow \infty$) by absence of memory ($\alpha = 1$) a strong dependence of the variance $\sigma_{xx}(t)$ on the magnetic field, which contrasts with the case of $\alpha < 1$, where at $t \rightarrow \infty$ the influence of the magnetic field on $\sigma_{xx}(t)$ is negligible.

In the long-time limit the asymptotic mean angular momentum $\langle L_z \rangle_{as}$ is convenient to present as a sum of two contributions:

$$\langle L_z \rangle_{as} = \langle L_z \rangle_1 + \langle L_z \rangle_2, \quad (31)$$

where the first part $\langle L_z \rangle_1$ corresponds to the case without noise and the second part $\langle L_z \rangle_2$ characterizes the noise-induced angular momentum. According to Eqs. (15), (16), (20), and (21) we can obtain $\langle L_z \rangle_1$, which we write as [see also Eq. (A3)]

$$\langle L_z \rangle_1 = \frac{A_0^2}{\Omega} |\hat{H}_{32}(-i\omega)|^2 \left[\omega_0^2 - \omega^2 + \gamma \omega^\alpha \cos\left(\frac{\pi\alpha}{2}\right) \right]. \quad (32)$$

The noise-induced angular momentum $\langle L_z \rangle_2$ is obtained from Eqs. (20) and (21), yielding the following result:

$$\langle L_z \rangle_2 = 2 \int_0^\infty [\dot{H}_{32}(t)M_1(t) - \dot{H}_{12}(t)M_3(t)]dt, \quad (33)$$

where the functions $M_1(t)$ and $M_3(t)$ are determined by Eq. (24). Another representation of $\langle L_z \rangle_2$, more convenient for numerical calculations, is given by Eq. (B3) in Appendix B. It is remarkable that the formulas (32) and (33) are applicable also in the case without a trapping potential ($\omega_0 = 0$) if the condition

$$\alpha < \frac{2}{3} + \frac{\delta}{3} \quad (34)$$

is fulfilled. Particularly, in the case of an internal noise $\delta = \alpha$ this condition is valid for all values of the memory exponent $0 < \alpha < 1$.

It is important to note that in the case of an internal noise the noise-induced angular momentum $\langle L_z \rangle_2$ vanishes for all values of other system parameters (see also Appendix C):

$$\langle L_z \rangle_2 = 0, \quad \delta = \alpha. \quad (35)$$

Thus, in the general case $\xi(t) = \xi^{(1)}(t) + \xi^{(2)}(t)$ the asymptotic mean angular momentum $\langle L_z \rangle_{as}$ is independent of the temperature T .

III. RESULTS

A. Distribution of the particle position

As the right-hand sides of Eqs. (7) and (8) are Gaussian processes $\xi(t) = [\xi_1(t), \xi_2(t)]$, $\mathbf{r}(t) = [X(t), Y(t)]$ is also Gaussian and therefore completely specified by its mean and correlation matrix. So in the long-time limit, $t \rightarrow \infty$, the particle position distribution $P(\mathbf{r})$ is Gaussian [see also Eqs. (22) and (23)]:

$$P(\mathbf{r}, t) = \frac{1}{2\pi\sigma_{xx}(\infty)} \exp\left[-\frac{1}{2\sigma_{xx}(\infty)}(\Delta X^2 + \Delta Y^2)\right], \quad (36)$$

where

$$\Delta X \equiv X - \langle X(t) \rangle, \quad \Delta Y \equiv Y - \langle Y(t) \rangle, \quad (37)$$

and the averages $\langle X(t) \rangle$ and $\langle Y(t) \rangle$ are determined by Eqs. (15) and (16). Since the mean position $\langle \mathbf{r}(t) \rangle$ of the particles is described by an ellipse in the xy plane, the distribution $P(\mathbf{r}, t)$ is characterized by an ellipsoidal band with an effective width $2\sqrt{\sigma_{xx}}$ around the origin of coordinates (see Fig. 1). The lengths C_1 and C_2 of the principal axes of the elliptical distribution and their orientation in space are determined by

$$C_{1,2}^2 = \frac{1}{2} \left[A_x^2 + A_y^2 \pm \sqrt{(A_x^2 - A_y^2)^2 + 4A_x^2 A_y^2 \cos^2(\varphi_1 - \varphi_3)} \right], \quad (38)$$

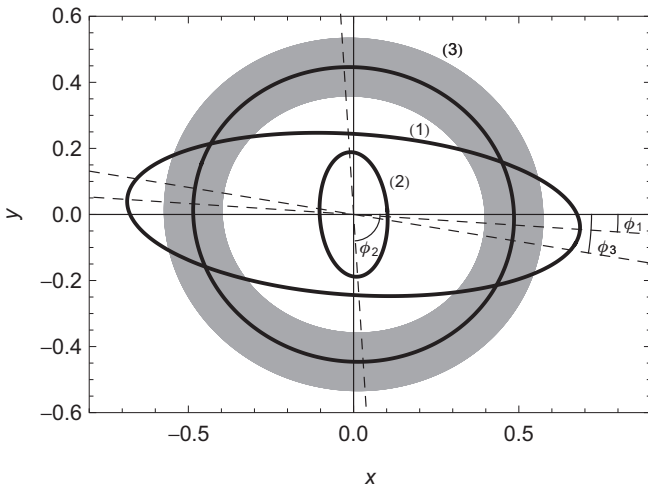


FIG. 1. The mean position $\langle \mathbf{r}(t) \rangle$ of particles (ellipsoids) in the xy plane computed from Eqs. (15)–(17), (A2), and (A3) in the long-time limit, $t \rightarrow \infty$. Parameter values: $\omega_0 = x_0 = y_0 = 0$, $\gamma = 2$, $\alpha = 0.1$, and $\Omega = 3$. Line (1), $\omega = 0.2$; line (2), $\omega = 2.5$; line (3), $\omega = 3.85$. The angles between the major axis and the x axis are $\phi_1 \approx -0.066$, $\phi_2 \approx -1.506$, $\phi_3 \approx -0.163$. The shaded ellipsoidal band with a width of $\sqrt{2\sigma_{xx}} \approx 0.089$ around curve (3) characterizes the variance σ_{xx} computed from Eq. (B1) at the noise parameter values $\delta = 0.6$ and $D = 0.002$.

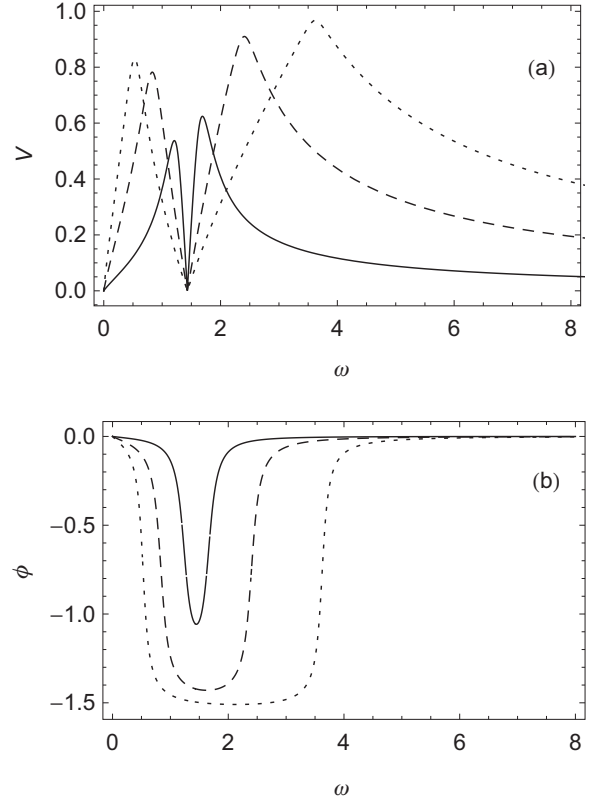


FIG. 2. The ratio $V = C_2/C_1$ of the minor and the major axis of the particles position ellipsoid and the angle ϕ between the major axis and x axis as functions of the driving frequency ω . The curves are computed from Eqs. (A2), (A3), and (38)–(40) for several values of the Larmor frequency Ω . Parameter values: $\omega_0 = 0$, $\alpha = 0.1$, $A_0 = 1$, and $\gamma = 2$. Solid line, $\Omega = 0.4$; dashed line, $\Omega = 1.5$; dotted line, $\Omega = 3$.

and

$$\tan \phi = \frac{A_x A_y \cos(\varphi_1 - \varphi_3)}{C_1^2 - A_y^2}, \quad (39)$$

where ϕ denotes the angle between the major axis with length C_1 and the x axis, the subscript 1 (2) refers to the plus (minus) sign, and

$$A_x = A_0 |\hat{H}_{12}(-i\omega)|, \quad A_y = A_0 |\hat{H}_{32}(-i\omega)|. \quad (40)$$

In Fig. 2 we depict, on two panels, the behavior of the ratio $V = C_2/C_1$ of the minor and major axes of the distribution ellipsoid (an isotropy parameter of the distribution) and the angle ϕ versus the driving parameter ω . Both $V(\omega)$ and $\phi(\omega)$ exhibit a nonmonotonic dependence on ω , i.e., a typical resonance phenomenon occurs as ω increases. An interesting peculiarity of Fig. 2(a) is the double resonant peak structure of the isotropy parameter V versus the frequency ω . The effect is very pronounced at low values of the memory exponent α . To throw some light on the physics of this effect we shall now briefly consider the behavior of $V(\omega)$ in the parameter regime $\alpha \rightarrow 0$. In this case, from Eqs. (38), (40), (A2), and (A3) it follows that the function $V(\omega)$ reaches three local extrema:

two maxima $V_{\max}(\omega) = 1$ at

$$\omega_{1,2} = \sqrt{\omega_0^2 + \gamma + \frac{\Omega^2}{4}} \pm \frac{\Omega}{2}, \quad (41)$$

where the indices 1 and 2 refer to the plus and minus sign, respectively, and one local minimum $V_{\min}(\omega) = 0$ at

$$\omega_m = \sqrt{\omega_0^2 + \gamma}. \quad (42)$$

From Eq. (41) it is seen that for sufficiently large values of the Larmor frequency Ω , the position of the first minimum (ω_1) grows in proportion to Ω and the position of the second maximum (ω_2) tends to zero. The behavior of the particles position ellipsoid is characterized by the following scenario. For small values of the driving frequency $\omega \approx 0$, the major axis of the ellipse is finite as

$$C_1 \approx \frac{A_0}{\gamma + \omega_0^2}, \quad \omega \rightarrow 0, \quad (43)$$

and oriented along the x axis, $\phi \approx 0$, but $C_2 \approx 0$, i.e., the isotropy parameter $V \approx 0$. By increasing ω , both C_1 and C_2 increase up to very large values and the ellipse turns into a circle, $V = 1$, at $\omega = \omega_2$. In this case the angle ϕ tends to $-\pi/4$. By further increase of ω , the anisotropy of particle distribution grows and the major axis of the ellipse aligns more and more with the y axis. At $\omega = \omega_m$ the ellipse reduces to a line with $C_2 \approx 0$, $\phi = -\pi/2$, and

$$C_1 \approx \frac{A_0}{\Omega \sqrt{\gamma + \omega_0^2}}, \quad \omega \rightarrow \omega_m. \quad (44)$$

In the interval $\omega \in (\omega_m, \omega_1)$ the particles position distribution gets more isotropic again and at $\omega = \omega_1$ the ellipse is characterized by $C_1 \approx C_2 \rightarrow \infty$, $V \approx 1$, and $\phi = -\pi/4$, i.e., it has become a circle. Finally, if $\omega > \omega_1$, the ellipse begins to stretch along the major axis and aligns more and more with the x axis as the driving frequency ω increases (the anisotropy grows). In the limit $\omega \rightarrow \infty$ the angle ϕ tends to zero and the ellipse reduces to a point $C_1 \sim 1/\omega^2 \rightarrow 0$, $C_2 \sim 1/\omega^3 \rightarrow 0$. It is remarkable that the scenario described above is similar to the one for the ordinary charged oscillator without a friction term in the external electromagnetic field. This is a manifestation of the cage effect, which is due to the viscoelastic memory kernel present in our model. Namely, for small values of the memory exponent α , the friction force induced by a viscoelastic medium is not just slowing down the particle but also causing the particle to undergo a rattling motion, which can be explained by the harmonic motion of the particle in a cage formed by the surrounding particles [15,21]. In this case, at small α the medium is binding the particle, preventing dissipation but forcing elastic oscillations.

Formulas (38)–(40) are exactly the same as can be derived for an ordinary charged oscillator (without memory, $\alpha = 1$) if we replace the eigenfrequency ω_0 and the friction coefficient γ with the corresponding effective quantities $\omega_{0\text{ef}}$ and γ_{ef} :

$$\begin{aligned} \omega_{0\text{ef}}^2 &= \omega_0^2 + \gamma \omega^\alpha \cos\left(\frac{\alpha\pi}{2}\right), \\ \gamma_{\text{ef}} &= \gamma \omega^{\alpha-1} \sin\left(\frac{\alpha\pi}{2}\right). \end{aligned} \quad (45)$$

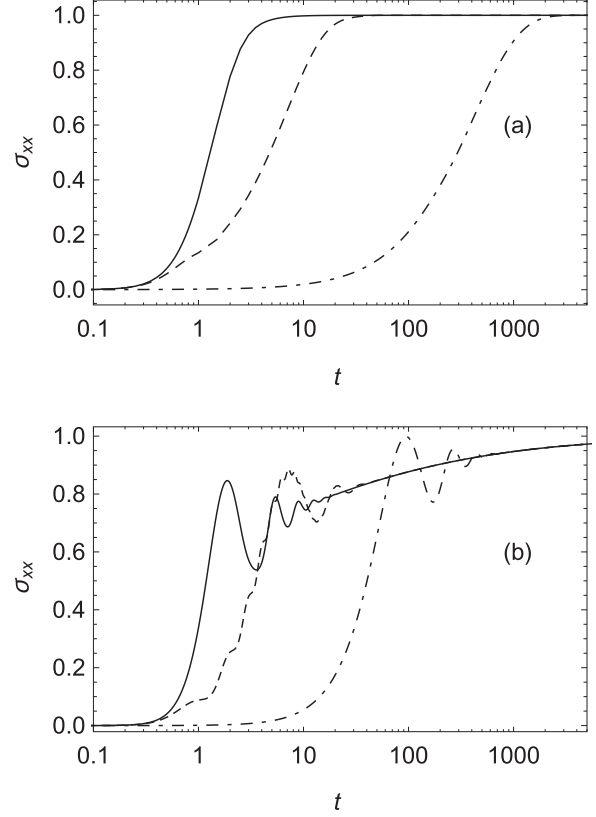


FIG. 3. Dependence of the variance $\sigma_{xx}(t)$ on time t , computed from Eqs. (A8), (A9), and (C1) in the case of an internal noise. System parameter values: $k_B T = 1$, $\gamma = 2$, and $\omega_0 = 1$. Solid line, $\Omega = 0.1$; dashed line, $\Omega = 5$; dash-dotted line, $\Omega = 50$. (a) The case of low memory, $\alpha = 0.9$. (b) The case of strong memory, $\alpha = 0.25$. In the limit $t \rightarrow \infty$ the variance tends to the equilibrium value 1.

Thus, in this context, our model (with memory) is equivalent to an oscillator without memory, but with the effective parameters (45). From Eqs. (45) it can be easily seen that by decreasing α the effective eigenfrequency increases and the effective friction coefficient decreases, thus demonstrating the increasing role of elastic friction. For example, in terms of the effective parameters γ_{ef} and $\omega_{0\text{ef}}$ from the behavior of the model without memory ($\alpha = 1$), it follows that the value of the driving frequency ω at which the isotropy parameter V vanishes (i.e., the ellipse reduces to a line) is independent of the magnetic field and is determined by the equation

$$\omega^2 = \omega_{0\text{ef}}^2 = \omega_0^2 + \gamma \omega^\alpha \cos\left(\frac{\alpha\pi}{2}\right). \quad (46)$$

Now we consider the asymptotic evolution of the variance $\sigma_{xx}(t)$ at large values of the time $t \gg (\gamma/\omega_0^2)^{1/\alpha}$. The behavior of an internal noise generated variance $\sigma_{xx}(t)$ by the presence of a trapping potential, $\omega_0 \neq 0$, is shown in Fig. 3 for certain values of the magnetic field and the memory exponent α .

It is important to note that although the temporal process of the relaxation of $\sigma_{xx}(t)$ to the equilibrium value depends on the Larmor frequency Ω and on the memory exponent α , the

asymptotic value of $\sigma_{xx}(t)$ at $t \rightarrow \infty$

$$\sigma_{xx}(\infty) = \frac{k_B T}{\omega_0^2} \quad (47)$$

only depends on the temperature T of the heat bath and on the stiffness of the trapping potential [see also Eq. (C3)]. Particularly, the relaxation process gets more rapid as the memory exponent α increases or as the Larmor frequency Ω decreases.

Henceforth our interest is focused on the case of an external noise, i.e., the internal noise $\xi^{(1)}(t)$ in Eq. (4) is absent. To avoid misunderstandings we emphasize here that the genuine asymptotic value of the variance $\sigma_{xx}^{(s)}(\infty)$ is the sum of an external noise generated part $\sigma_{xx}(\infty)$ and an internal noise generated part:

$$\sigma_{xx}^{(s)}(\infty) = \sigma_{xx}(\infty) + \frac{k_B T}{\omega_0^2}. \quad (48)$$

In the case of memory-induced trapping, $\omega_0 = 0$, the asymptotic behavior of $\sigma_{xx}^{(s)}(t)$ is always subdiffusive [see Eq. (C4)], but if the intensity D of the external noise is much larger than the intensity $k_B T \gamma$ of thermal noise and if the observation time t satisfies the inequality

$$t \ll \gamma^{-\frac{1}{2-\alpha}} \left(\frac{D}{k_B T \gamma} \right)^{\frac{1}{\alpha}} \quad (49)$$

the evolution of $\sigma_{xx}^{(s)}(t)$ in time is mainly determined by the external noise.

Figures 4 and 5 show, at various values of memory and noise exponents, the typical forms of the variance $\sigma_{xx}(\infty)$ versus the Larmor frequency Ω [see Eqs. (23) and (B1)]. In Fig. 4(a) the case of memory-induced trapping ($\omega_0 = 0$) for various values of the noise exponent $\delta > 2\alpha$ is considered. It is seen that at sufficiently large values of the Larmor frequency Ω , by increasing Ω the variance $\sigma_{xx}(\infty)$ decays monotonically. In this regime, for increasing δ the main effect consists in a more rapid decrease of σ_{xx} versus Ω . More precisely, at $2\alpha < \delta < 1$ it follows from Eq. (B1) that for large Ω the variance decays as a power law

$$\sigma_{xx} \approx \frac{D}{\gamma^2} \left(\frac{\gamma}{\Omega} \right)^{\frac{\delta-2\alpha}{1-\alpha}} \chi(\alpha, \delta), \quad \Omega \rightarrow \infty, \quad (50)$$

where the function $\chi(\alpha, \delta)$ depends only on the exponents α and δ , e.g.,

$$\begin{aligned} \chi(\alpha, \delta) &\approx \frac{2}{\pi\alpha} \sin\left(\frac{\pi\delta}{2}\right), \quad \delta \gg 2\alpha, \\ \chi(\alpha, \delta) &\sim \frac{2 \sin(\pi\alpha)}{\pi(\delta - 2\alpha)}, \quad \delta \rightarrow 2\alpha. \end{aligned} \quad (51)$$

It should be noted that in the vicinity of the critical value of the noise exponent, $\delta \approx \delta_c = 2\alpha$, the asymptotic formula (50) is invalid, since at $\delta = 2\alpha$ the system becomes unstable, i.e., σ_{xx} tends to infinity. For moderate and small values of Ω , $\Omega \lesssim \gamma^{\frac{1}{2-\alpha}}$, the curves in Fig. 4(a) demonstrate a nonmonotonic dependence on δ , thus indicating that a stochastic resonance occurs as the noise exponent increases. This phenomenon contrasts, in the regime $\delta > 2\alpha$, with the behavior of the model

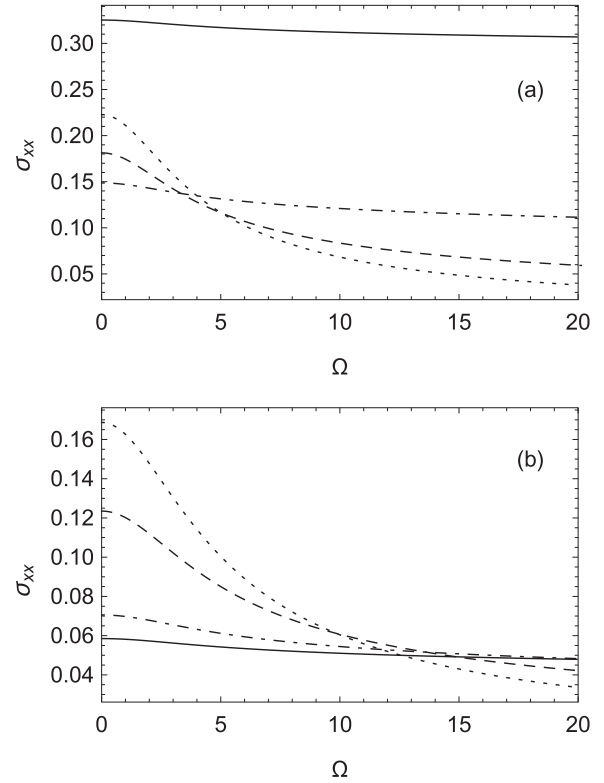


FIG. 4. The variance σ_{xx} vs the Larmor frequency Ω computed from Eq. (B1) at various values of the noise exponent δ . System parameter values: $\gamma = 2$, $\alpha = 0.1$, and $D = 0.1$. Solid line, $\delta = 0.22$; dot-dashed line, $\delta = 0.3$; dashed line, $\delta = 0.6$; dotted line, $\delta = 0.9$. (a) The case of memory-induced trapping, $\omega_0 = 0$. (b) $\omega_0 = 1$. Note the nonmonotonic dependence of σ_{xx} on δ in panel (a).

with external trapping, $\omega_0 \neq 0$, where such an effect is absent [see Fig. 4(b)]. Figure 5 depicts, in the case of external trapping, the typical dependence of σ_{xx} on Ω for various values of the

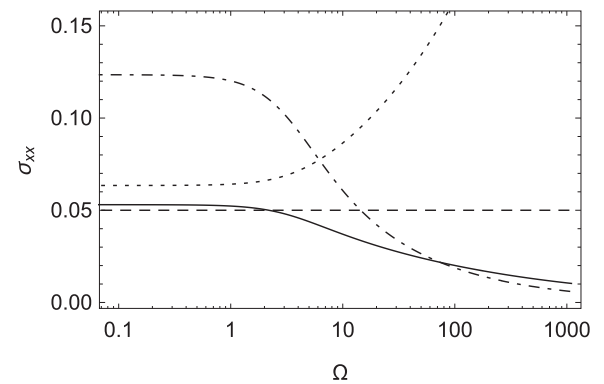


FIG. 5. A plot of the dependence of the variance σ_{xx} on the Larmor frequency Ω at various values of the memory exponent α . The curves are computed from Eq. (B1). Parameter values: $\omega_0 = 1$, $\gamma = 2$, $D = 0.1$, and $\delta = 0.6$. Dot-dashed line, $\alpha = 0.1$; solid line, $\alpha = 0.3$; dashed line, $\alpha = 0.6$; dotted line, $\alpha = 0.9$. Note that in the case of an internal noise (dashed line) the variance σ_{xx} is independent of the Larmor frequency Ω .

memory exponent α . Depending on the parameters α and δ the following three characteristic regimes can be discerned.

(i) If the noise exponent δ is larger than the memory exponent α , $\delta > \alpha$, then σ_{xx} is a monotonically decaying function on the Larmor frequency Ω .

(ii) If $\delta = \alpha$, the system is subjected to an internal noise and consequently the variance σ_{xx} is independent of Ω , being determined by the temperature of a heat bath instead.

(iii) In the case of $\delta < \alpha$, contrary to the regime $\delta > \alpha$, the variance σ_{xx} increases monotonically as Ω increases. For example, if $\alpha = 1$, the asymptotic behavior of σ_{xx} is described by the following equation:

$$\sigma_{xx} \approx \frac{D\Omega^{1-\delta}}{\gamma\omega_0^{2(2-\delta)}} \sin\left(\frac{\pi}{2}\delta\right), \quad \Omega \rightarrow \infty. \quad (52)$$

So, for the system without memory an increase of the particles position variance by increasing Ω is expected at any value of the noise exponent ($\delta < 1$) from Eq. (52). Those findings may be suggestive of some new possibilities for designing plasma devices, since, in the case of $\delta > \alpha$, an increase in the strength of the magnetic field can significantly suppress the external noise generated part of the spatial dispersion of charged particles.

Moreover, the graphs in Fig. 5 indicate a stochastic resonancelike suppression of σ_{xx} versus the memory exponent α with a local minimum of σ_{xx} at $\alpha < \delta$. Let us mention that we use the term stochastic resonance in a wide sense, meaning a nonmonotonic behavior of the moments of the output process in response to the noise parameters [7,12]. The stochastic resonancelike suppressions of σ_{xx} versus δ and α at various values of Ω are illustrated in Figs. 6(a) and 6(b), respectively. In the case of $\omega_0 = 0$, exposed in Fig. 6(a), the effect is more pronounced at small values of the Larmor frequency. At sufficiently large values of Ω , $\Omega \gg \gamma^{\frac{1}{2-\alpha}}$, the effect disappears. Such behavior of the variance σ_{xx} versus the noise exponent δ contrasts with the phenomenon of memory-induced resonancelike suppression of σ_{xx} at intermediate values of the memory exponent α for the model with external trapping, $\omega_0 \neq 0$ [see Fig. 6(b)]. In the latter case the effect gets more and more pronounced as the Larmor frequency Ω increases [see also Eq. (52)]. Finally, we note that in the limit $\alpha \rightarrow 0$ the variance σ_{xx} increases rapidly to infinity, thus expressively demonstrating the cage effect: in this limit, due to the cage effect, the effective damping (friction) coefficient tends to zero and the fractional derivative in Eqs. (7) and (8) acts like an elastic force.

B. Angular momentum

Our next task is to examine the mean angular momentum $\langle L_z \rangle_{as}$ of charged particles in the electromagnetic field [see also Eqs. (31)–(33)]. To discern the effects caused by an additive external periodic force and a noise in the behavior of $\langle L_z \rangle_{as}$, we will in the first place consider the corresponding components $\langle L_z \rangle_1$ and $\langle L_z \rangle_2$ in Eq. (31) separately. Since in the case of internal noise the noise-induced part $\langle L_z \rangle_2$ of the mean angular momentum vanishes [see Eq. (35)], in the general case the behavior of $\langle L_z \rangle_{as}$ only depends on the internal noise indirectly through the memory kernel $\eta(t)$ in Eq. (1). Thus, without loss of generality we can restrict our attention to the case

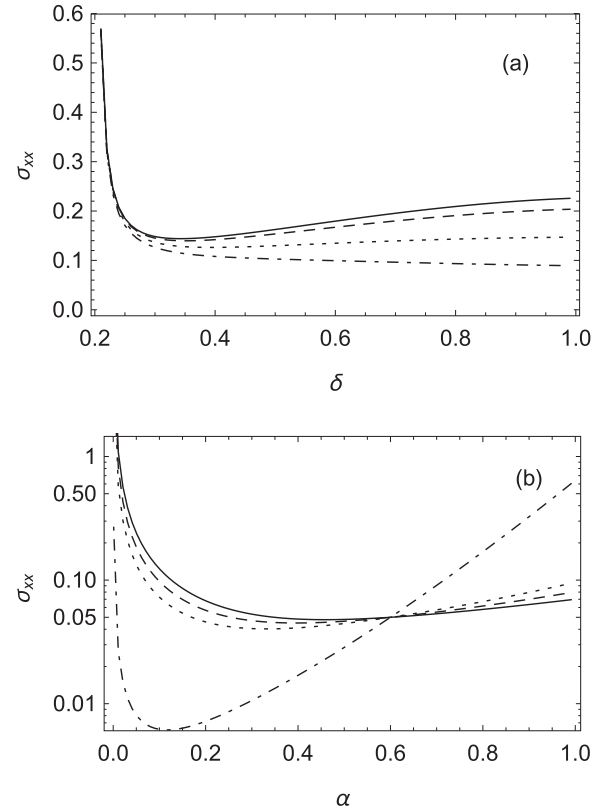


FIG. 6. The dependence of the variance σ_{xx} on the noise exponent δ and on the memory exponent α computed from (B1). Parameter values: $D = 0.1$ and $\gamma = 2$. (a) The variance σ_{xx} vs δ at $\omega_0 = 0$ and $\alpha = 0.1$. Solid line, $\Omega = 0.5$; dashed line, $\Omega = 1.5$; dotted line, $\Omega = 3.5$; dash-dotted line, $\Omega = 7$. Note that at the critical value of the noise exponent $\delta_c = 2\alpha = 0.2$ the variance σ_{xx} tends to infinity, i.e., at $\delta \leq \delta_c$ the system is unstable. (b) σ_{xx} vs α at $\omega_0 = 1$ and $\delta = 0.6$. Solid line, $\Omega = 0.1$; dashed line, $\Omega = 3.5$; dotted line, $\Omega = 7$; dash-dotted line, $\Omega = 1000$. In the limit $\alpha \rightarrow 0$ the variance σ_{xx} tends to infinity. Note that at $\alpha = 0.6$ all curves intersect, demonstrating that in the case of an internal noise ($\delta = \alpha$) the variance σ_{xx} is independent of the Larmor frequency Ω [see Eq. (47)].

of external noise, $\xi(t) = \xi^{(2)}(t)$. In Fig. 7 we depict, on two panels, the typical forms of the graphs $\langle L_z \rangle_1$ and $\langle L_z \rangle_1$ at various values of the Larmor frequency Ω and the driving frequency ω , respectively. Here we emphasize once again that $\langle L_z \rangle_1$ is independent of noise parameters (except the memory exponent α).

Two effects can be discerned from the graphs exposed in Fig. 7. First, the sign reversals of $\langle L_z \rangle_1$ versus ω . Relying on Eq. (32) one can establish the emergence of sign reversals of $\langle L_z \rangle_1$ due to system parameter variations. Namely, a negative $\langle L_z \rangle_1$ appears for the parameter values determined by the equation

$$\omega^2 - \gamma\omega^\alpha \cos\left(\frac{\pi}{2}\alpha\right) - \omega_0^2 > 0. \quad (53)$$

From Eq. (53) it follows that sign reversals can be controlled by varying the frequency of the electric field, the memory exponent α , and even the friction coefficient γ . Comparing Eq. (53) with Eq. (46) we see that at the point of a sign

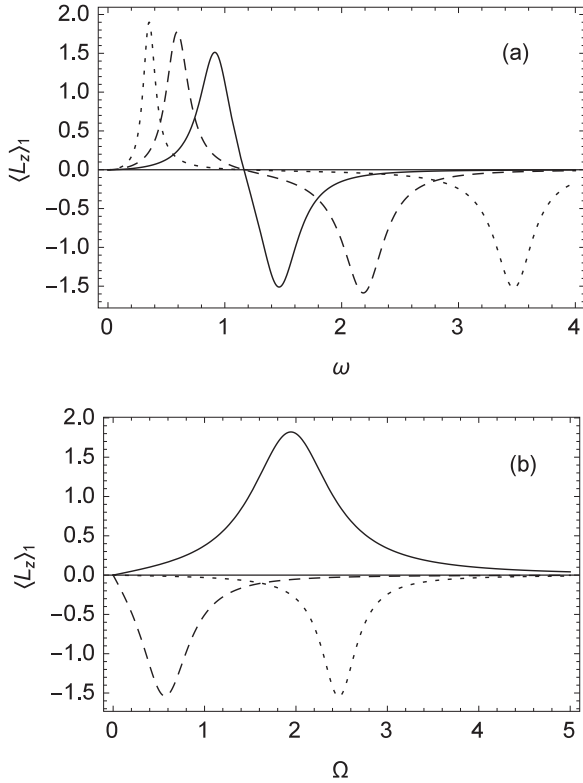


FIG. 7. Resonance of the noise-independent component $\langle L_z \rangle_1$ of the mean angular momentum [see Eq. (32)] in the case of external trapping, $\omega_0 = 1$. System parameter values: $\gamma = 0.5$, $A_0 = 1$, and $\alpha = 0.55$. (a) $\langle L_z \rangle_1$ vs the driving frequency ω at various values of the Larmor frequency Ω . Solid line, $\Omega = 0.5$; dashed line, $\Omega = 1.5$; dotted line, $\Omega = 3.0$. (b) $\langle L_z \rangle_1$ vs Ω at various values of ω . Solid line, $\omega = 0.5$; dashed line, $\omega = 1.5$; dotted line, $\omega = 3.0$.

reversal of $\langle L_z(\omega) \rangle_1$ the isotropy parameter $V(\omega)$ of the mean trajectory of the particle tends to zero. Thus, in this case the particles position ellipse reduces to a line and consequently the mean position behaves as a one-dimensional oscillator subjected to a periodic force. It is important to note that this phenomenon also occurs in the case without external trapping, $\omega_0 = 0$. This contrasts with the case of Stokes friction ($\alpha = 1$, i.e., without memory), where such an effect at $\omega_0 = 0$ is absent. Thus, in some cases the sign reversals of the mean angular momentum can give an indicator to estimate the viscoelastic properties of the medium in possible experiments. Second, a multiresonance of $\langle L_z \rangle_1$ versus ω and a resonance of $\langle L_z \rangle_1$ versus the Larmor frequency Ω appear. Although the dependence of the positions and height of resonance peaks on system parameters is generally very complicated and thus the corresponding formulas are lengthy and not transparent, it is possible to find simple analytical results for some particular cases. In particular, for the case $\omega = \omega_0$ we obtain that the position of the resonance peak of $\langle L_z(\Omega) \rangle_1$ is determined by

$$\Omega_{\text{ex}} = \frac{\gamma}{\omega_0^{1-\alpha} \sqrt{3}} \sqrt{\cos(\alpha\pi) + \sqrt{3 + \cos^2(\alpha\pi)}}. \quad (54)$$

The corresponding extreme value of the mean angular momentum reads as

$$\langle L_z(\Omega_{\text{ex}}) \rangle_1 = \frac{A_0^2 \omega_0^{1-2\alpha} \sqrt{3}}{8\gamma^2 \sin(\frac{\pi}{2}\alpha) \sin(\pi\alpha)} \times \left[1 + \frac{\cos(\pi\alpha)}{\sqrt{\cos(\pi\alpha) + \sqrt{3 + \cos^2(\pi\alpha)}}} \right]. \quad (55)$$

Evidently, the maximum of $\langle L_z(\Omega) \rangle_1$ increases and the position of the resonance peak Ω_{ex} shifts to smaller values of the Larmor frequency as the friction coefficient γ decreases. The dependence of $\langle L_z(\Omega_{\text{ex}}) \rangle_1$ on the memory exponent α is more interesting. In the case without memory, $\alpha = 1$, the resonance versus Ω is absent, i.e., $\langle L_z(\Omega_{\text{ex}}) \rangle_1 = 0$. If α decreases, the height of the resonance peak increases monotonically and the position of the peak is shifted from $\Omega_{\text{ex}} = \frac{\gamma}{\sqrt{3}}$ at $\alpha \approx 1$ to $\Omega_{\text{ex}} = \gamma/\omega_0$ at $\alpha = 0$. Notably, at strong memory, $\alpha \rightarrow 0$, the height of the peak tends to infinity, which is in accordance with the fact that, due to the cage effect, an effective friction coefficient tends to zero at $\alpha = 0$. Here we emphasize that in this regime, $\omega = \omega_0$, the resonance $\langle L_z \rangle_1$ versus Ω is a memory-induced effect, since in the case without memory $\langle L_z \rangle_1$ is always zero.

Differently from $\langle L_z \rangle_1$, the noise-induced part $\langle L_z \rangle_2$ of the mean angular momentum $\langle L_z \rangle_{\text{as}}$ [see Eq. (31)] is independent of the driving frequency ω . From Eqs. (33) and (B3), there follows the somewhat surprising circumstance that the dependence of $\langle L_z \rangle_2$ on the Larmor frequency Ω is qualitatively different for the regimes $\delta > \alpha$ and $\delta < \alpha$ (see Fig. 8).

Although in both cases the function $\langle L_z(\Omega) \rangle_2$ exhibits a resonancelike nonmonotonic dependence on Ω , in the case $\delta > \alpha$ the local extremum of $\langle L_z \rangle_2$ is a minimum, but if the memory exponent α is larger than the noise exponent δ , $\alpha > \delta$, the local extremum is a maximum. The influence of the noise exponent δ is characterized by the following scenario: for small values of δ , $\delta < \alpha$, the maximum of $\langle L_z \rangle_2$ is positive and decreases as δ increases. At $\delta = \alpha$ the resonance disappears, $\langle L_z \rangle_2 = 0$. For further increasing values of δ , a negative resonant minimum of $\langle L_z \rangle_2$ appears, which gets more and more pronounced as δ tends to 1. Notably, in the case of an internal noise, i.e., $\delta = \alpha$, the noise-induced part of the mean angular momentum vanishes, $\langle L_z \rangle_2 = 0$, for any values of the other system parameters. As in both components, $\langle L_z \rangle_1$ and $\langle L_z \rangle_2$, of the mean angular momentum $\langle L_z \rangle_{\text{as}}$ [see Eqs. (31)–(33)] the resonance phenomena versus Ω are controlled by independent system parameters, such as the external driving frequency ω and amplitude A_0 for $\langle L_z \rangle_1$ and the noise parameters δ and D for $\langle L_z \rangle_2$, it is obvious that depending on the values of system parameters the dependence of the total angular momentum $\langle L_z \rangle_{\text{as}}$ on the Larmor frequency can exhibit a variety of multiresonance structures. The latter claim is illustrated in Fig. 9 at two parameter regimes.

Both graphs exhibit three local extrema and two sign reversals. The maximum in Fig. 9(a) corresponds to the resonance of $\langle L_z \rangle_1$ and the minima emerge as a result of the resonant behavior of $\langle L_z \rangle_2$; in the case exposed in Fig. 9(b) the situation is vice versa. This is in contrast with the case of an internal noise, $\delta = \alpha$, where the dependence of $\langle L_z \rangle_{\text{as}}$

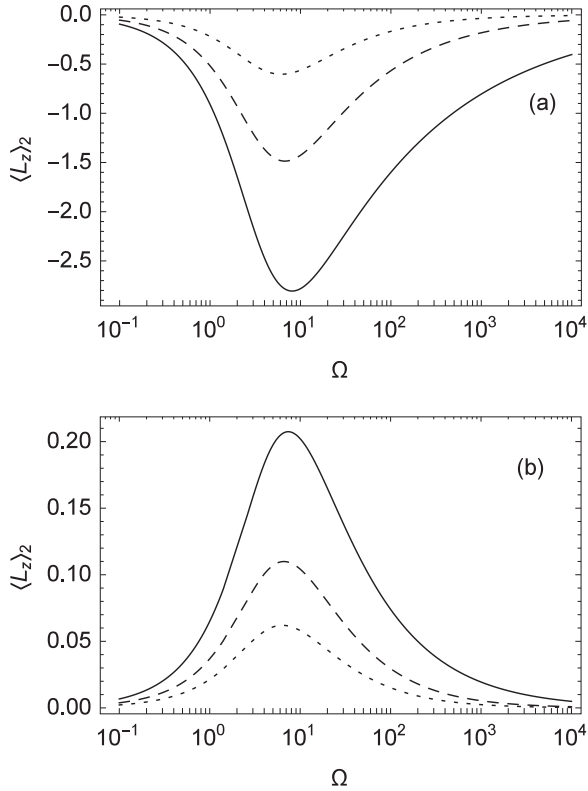


FIG. 8. Dependence of the noise-induced component $\langle L_z \rangle_2$ of the mean angular momentum [see Eqs. (31) and (33)] on the Larmor frequency Ω . System parameter values: $\omega_0 = 1$, $\gamma = 2.5$, and $D = 5$. (a) The case of $\delta > \alpha$, $\alpha = 0.2$. Solid line, $\delta = 0.9$; dashed line, $\delta = 0.7$; dotted line, $\delta = 0.5$. (b) The case of $\delta < \alpha$, $\delta = 0.4$. Solid line, $\alpha = 0.8$; dashed line, $\alpha = 0.6$; dotted line, $\alpha = 0.5$. At $\Omega \rightarrow \infty$, all curves tend to zero as a power law.

on Ω is always monomodal and sign reversals of the angular momentum versus Ω are absent.

The effects of resonance and sign reversals are not restricted to the dependencies of the angular momentum on Ω and ω , but also occur in the dependence of $\langle L_z \rangle_{as}$ on other system parameters, particularly on α .

Figure 10 depicts, at some parameter values, the memory-induced resonance and sign reversals for $\langle L_z \rangle_{as}$ versus the memory exponent α for systems with external trapping, $\omega_0 \neq 0$, and without trapping, $\omega_0 = 0$. At very strong memory, $\alpha \rightarrow 0$, in both systems $\langle L_z \rangle_{as}$ decreases, due to the cage effect, rapidly to $-\infty$, i.e., an instability occurs at $\alpha = 0$. All graphs $\langle L_z(\alpha) \rangle_{as}$ demonstrate memory-induced sign reversals at intermediate values of α . In the parameter regime corresponding to the dotted line in Fig. 10 the contribution of the noise independent component $\langle L_z \rangle_1$ in $\langle L_z \rangle_{as}$ is substantial, causing a resonancelike peak at relatively small values of α . For other curves in Fig. 10 the influence of $\langle L_z \rangle_1$ on the qualitative behavior of $\langle L_z(\alpha) \rangle_{as}$ is rather small and thus in these cases the behavior of $\langle L_z \rangle_{as}$ reflects mainly an interplay of colored noise and memory. Particularly, in the case without external trapping ($\omega_0 = 0$) the main difference from the case $\omega_0 \neq 0$ is the occurrence of a noise-induced instability, which causes a rapid unlimited increase of $\langle L_z \rangle_{as}$ at $\alpha \approx \alpha_{cr} = (2 + \delta)/3$ [see also Fig. 10(a)].

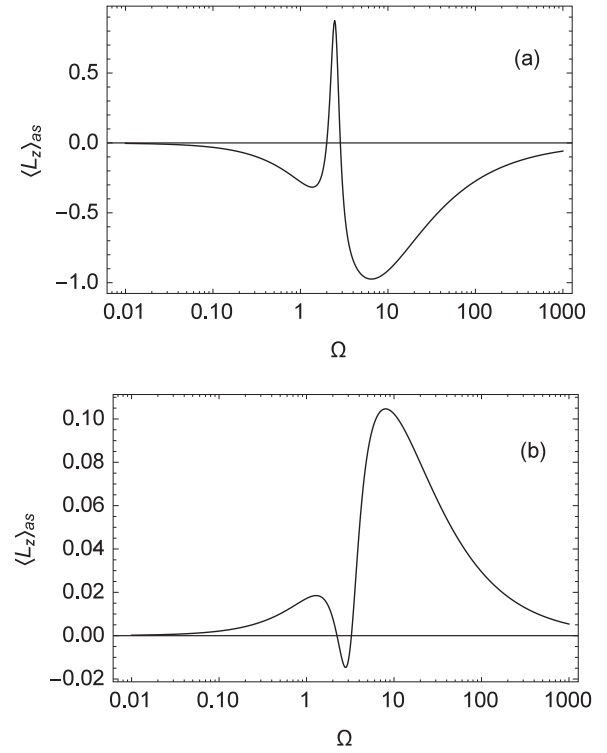


FIG. 9. Multiresonance of the particle mean angular momentum $\langle L_z \rangle_{as}$ vs the Larmor frequency Ω computed from Eqs. (31)–(33) at the time scaling $\omega_0 = 1$. System parameter values: $D = 5$, $\delta = 0.4$, and $\gamma = 2.5$. (a) The parameter regime: $\delta > \alpha$, $\omega = 1$, $\alpha = 0.1$, and $A_0 = 1$. (b) The parameter regime: $\alpha > \delta$, $\omega = 4$, $\alpha = 0.6$, and $A_0 = 1.5$.

IV. CONCLUSIONS

Motivated by studies of the dynamics of charged particles in plasmas in the presence of a magnetic field [3,37], we have considered the stochastic dynamics of a charged fractional oscillator with a power-law memory kernel under the action of crossed periodic electric field and a constant magnetic field. Fluctuations of the input, arising from particles interaction with environment, are expressed as an additive fractional Gaussian noise, which is assumed to be the sum of two uncorrelated contributions: an internal noise with an exponent α and an external noise with an exponent δ .

The main aim of the present paper was, using the GLE approach, to obtain the exact formulas for the output first-order and second-order statistical moments generated by the model considered. In the long-time limit, we have been able to derive exact analytical expressions of the particles' position distribution and the mean angular momentum.

As our main result we have established that in the investigated model an interplay of the memory, external periodic forcing, magnetic field, and colored noise effects can generate a rich variety of nonequilibrium phenomena, namely, (i) in the case of an external noise (i.e., without internal noise) the existence of the critical memory exponent $\alpha_{cr} = 0.5$ for an externally unbounded particle, which marks, by certain conditions for the noise exponent δ [see Eq. (28)], a dynamical transition from the confined dynamics of the particle to the subdiffusive (or superdiffusive) regime; (ii) a memory-induced

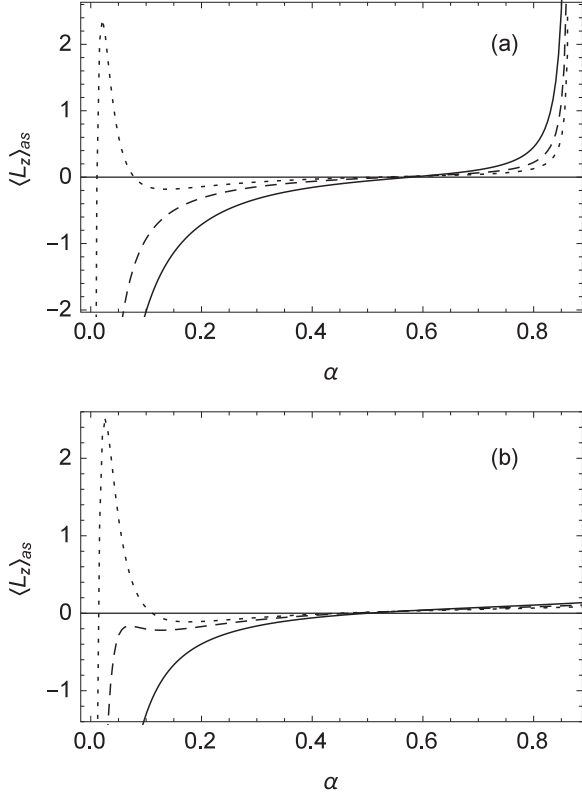


FIG. 10. The mean angular momentum $\langle L_z \rangle_{as}$ as a function of the memory exponent α computed from Eqs. (31), (32), and (B3). The system parameter values: $\omega = 1$; $\Omega = 3.8$, $\delta = 0.6$, $A_0 = 1.5$, $D = 5$. (a) The case of memory-induced trapping, $\omega_0 = 0$; solid line, $\gamma = 3$; dashed line, $\gamma = 4$; dotted line, $\gamma = 5$. (b) The case of external harmonic trapping, $\omega_0 = 1$; solid line, $\gamma = 3$; dashed line, $\gamma = 3.5$; dotted line, $\gamma = 4$. Note that in panel (a) the mean angular momentum tends to infinity at the critical value α_{cr} of the memory exponent, $\alpha_{cr} \approx 0.867$. All curves tend to $-\infty$ at $\alpha = 0$.

strong resonancelike suppression of the particles spatial dispersion at intermediate values of the memory exponent α in the case of high values of the Larmor frequency Ω ; (iii) a multi-resonance-like behavior of the anisotropy in the particle position distribution versus the driving frequency, implying

that it can be efficiently excited by an oscillating external force, even in the case without external trapping; (iv) multiresonance and sign reversals of the mean angular momentum $\langle L_z \rangle_{as}$ of charged particles versus the driving frequency, versus the Larmor frequency, and even versus the memory exponent; and (v) by the presence of a trapping potential the existence of three qualitatively different behaviors of the particles position variance σ_{xx} versus Ω , depending on the values of the exponent of an external noise $0 < \delta < 1$: if $\delta > \alpha$, then by increasing Ω , the variance σ_{xx} decreases to an equilibrium value determined by an internal noise; if $\delta = \alpha$, i.e., in the case of an internal noise, σ_{xx} is independent of Ω and α ; for $\delta < \alpha$, the variance σ_{xx} increases as Ω increases. This contrasts with the case of Stokes friction ($\alpha = 1$), where σ_{xx} always increases (or remains constant at $\delta = 1$) by increasing Ω . Moreover, another important effect, perhaps also from an experimental point of view, is the sign reversals of $\langle L_z \rangle_{as}$ by increasing Ω . Since in the case of internal noise such sign reversals are absent, the emergence of a sign reversal of $\langle L_z \rangle_{as}$ by a variation of the Larmor frequency is an indication of the domination of external noise in the random input.

We believe that the results of this paper not only supply material for theoretical investigations of fractional dynamics in stochastic systems but also suggest some possibilities for interpreting experimental data, especially in the field of plasmas [32–35,38]. A further detailed study is, however, necessary, especially an investigation of the behavior of second moments in the case of more general internal noises, e.g., a Mittag-Leffler noise with a characteristic memory time for the memory kernel [47,48]

Finally, according to the results of Ref. [20], we speculate that the model discussed in this paper can be expanded to one suitable for studying systems with an additional multiplicative noise (e.g., for systems in a fluctuating magnetic field).

ACKNOWLEDGMENTS

This paper was supported by the International Atomic Energy Agency Coordinated Research Project (CRP) F13016 Grant No. RC-20428, and by the European Union through the European Regional Development Fund. The authors would like to thank the anonymous reviewers for their valuable comments.

APPENDIX A: FORMULAS FOR THE RELAXATION FUNCTIONS

1. Laplace transforms of the relaxation functions

The relaxation functions $H_{ik}(t)$ in Eq. (12) can be obtained by means of the Laplace transformation technique. From Eqs. (10)–(13) with the initial conditions

$$H_{ik}(0) = \delta_{ik}$$

we obtain the following system of algebraic linear equations for $\hat{H}_{ik}(s)$, i.e., for the Laplace transforms of $H_{ik}(t)$ [see Eq. (13)]:

$$\begin{aligned} s\hat{H}_{1k} - \hat{H}_{2k} &= \delta_{1k}, \\ \omega_0^2 \hat{H}_{1k} + (s + \gamma s^{\alpha-1})\hat{H}_{2k} - \Omega \hat{H}_{4k} &= \delta_{2k}, \\ s\hat{H}_{3k} - \hat{H}_{4k} &= \delta_{3k}, \\ \Omega \hat{H}_{2k} + \omega_0^2 \hat{H}_{3k} + (s + \gamma s^{\alpha-1})\hat{H}_{4k} &= \delta_{4k}, \end{aligned} \quad (\text{A1})$$

where $k = 1, \dots, 4$. The solution of Eqs. (A1) reads as

$$\hat{H}_{12}(s) = \frac{s^2 + \gamma s^\alpha + \omega_0^2}{D(s)}, \quad (\text{A2})$$

$$\hat{H}_{32}(s) = -\frac{s\Omega}{D(s)}, \quad (\text{A3})$$

$$\hat{H}_{11}(s) = \hat{H}_{33} = \frac{1}{s}[1 - \omega_0^2 \hat{H}_{12}(s)], \quad (\text{A4})$$

$$\hat{H}_{34}(s) = \frac{1}{s} \hat{H}_{22}(s) = \frac{1}{s} \hat{H}_{44}(s) = -\frac{1}{\omega_0^2} \hat{H}_{21}(s) = -\frac{1}{\omega_0^2} \hat{H}_{43}(s) = \hat{H}_{12}(s), \quad (\text{A5})$$

$$\hat{H}_{14}(s) = \frac{1}{s} \hat{H}_{24} = -\frac{1}{s} \hat{H}_{42} = \frac{s}{\omega_0^2} \hat{H}_{31} = -\frac{s}{\omega_0^2} \hat{H}_{13}(s) = \frac{1}{\omega_0^2} \hat{H}_{41}(s) = -\frac{1}{\omega_0^2} \hat{H}_{23}(s) = -\hat{H}_{32}(s), \quad (\text{A6})$$

where

$$D(s) = (s^2 + \gamma s^\alpha + \omega_0^2)^2 + s^2 \Omega^2. \quad (\text{A7})$$

2. Time dependence of the relaxation functions

To evaluate the inverse Laplace transform of $\hat{H}_{ik}(s)$ [see Eqs. (A2)–(A7)] we use the residue theorem method described in Ref. [49]. As all other relaxation functions $H_{ik}(t)$ can be found from expressions for $H_{12}(t)$ and $H_{32}(t)$ with the help of simple time differentiation or integration we confine ourselves here to the relaxation functions $H_{12}(t)$ and $H_{32}(t)$. The inverse Laplace transform gives

$$H_{12}(t) = \frac{\gamma \sin(\pi\alpha)}{\pi} \int_0^\infty dr \frac{r^\alpha e^{-rt}}{\tilde{B}(r)} \{ \gamma^2 r^{2\alpha} - r^2 \Omega^2 + (r^2 + \omega_0^2)[r^2 + \omega_0^2 + 2\gamma r^\alpha \cos(\pi\alpha)] \} - \text{Re} \left[\frac{s_1 e^{s_1 t}}{C(s_1)} + \frac{s_2 e^{s_2 t}}{C(s_2)} \right], \quad (\text{A8})$$

$$H_{32}(t) = \frac{2\gamma\Omega \sin(\pi\alpha)}{\pi} \int_0^\infty dr \frac{r^{1+\alpha} e^{-rt}}{\tilde{B}(r)} [r^2 + \omega_0^2 + \gamma r^\alpha \cos(\pi\alpha)] + \text{Im} \left[\frac{s_1 e^{s_1 t}}{C(s_1)} + \frac{s_2 e^{s_2 t}}{C(s_2)} \right]. \quad (\text{A9})$$

Here s_1 and s_2 are the complex zeros of the equation

$$s^2 + \gamma s^\alpha + \omega_0^2 - i s \Omega = 0, \quad (\text{A10})$$

where Eq. (A10) is defined by the principal branch of s^α . The functions $\tilde{B}(r)$ and $C(s)$ are determined by

$$C(s) = 2\omega_0^2 + (2 - \alpha)\gamma s^\alpha - i s \Omega \quad (\text{A11})$$

and

$$\tilde{B}(r) = \left\{ [r^2 + \omega_0^2 + \gamma r^\alpha \cos(\pi\alpha)]^2 + \gamma^2 r^{2\alpha} \sin^2(\pi\alpha) + \Omega^2 r^2 \right\}^2 - 4\Omega^2 \gamma^2 r^{2(1+\alpha)} \sin^2(\pi\alpha). \quad (\text{A12})$$

The relaxation functions $H_{12}(t)$ and $H_{32}(t)$ can also be represented via a series of Mittag-Leffler-type special functions [43]. But as in the latter case the numerical calculations are very complicated, we suggest, apart from possible representations via Mittag-Leffler functions, a numerical treatment of Eqs. (A8)–(A12).

3. Asymptotic behavior of the relaxation functions

Now we present the behavior of the functions $H_{11}(t)$, $H_{12}(t)$, and $H_{32}(t)$ at a long-time limit ($t \rightarrow \infty$). The asymptotic behavior of $H_{ik}(t)$ is obtained from Eqs. (A2)–(A7) using the Tauberian theorem [50]:

$$H_{11}(t) = H_{33}(t) \sim \frac{\gamma}{\omega_0^2 \Gamma(1 - \alpha)} \times t^{-\alpha}, \quad (\text{A13})$$

$$H_{12}(t) \sim \frac{\alpha\gamma}{\omega_0^4 \Gamma(1 - \alpha)} \times t^{-(1+\alpha)}, \quad (\text{A14})$$

$$H_{32}(t) \sim \frac{2\alpha(\alpha + 1)\Omega\gamma}{\omega_0^6 \Gamma(1 - \alpha)} \times t^{-(2+\alpha)}. \quad (\text{A15})$$

Thus, at a long-time limit the relaxation functions $H_{ik}(t)$ decay as a power law. In the particular case of a “free” particle, i.e., without the harmonic trapping field, $\omega_0 = 0$, the asymptotic behavior of $H_{ik}(t)$ is different. Namely, at the long-time limit we obtain

$$H_{11}(t) = H_{33}(t) = 1, \quad (\text{A16})$$

$$H_{12}(t) \sim \frac{1}{\gamma \Gamma(\alpha)} t^{-(1-\alpha)}, \quad (\text{A17})$$

$$H_{32}(t) \sim \frac{(1-2\alpha)\Omega}{\gamma^2\Gamma(2\alpha)} t^{-2(1-\alpha)}. \quad (\text{A18})$$

From Eqs. (A16) and (12) it follows that in this case the mean position of the free particle depends strongly on the initial position, even by $t \rightarrow \infty$.

APPENDIX B: INTEGRALS FOR SECOND MOMENTS

Here the exact formulas for calculations of the variance σ_{xx} and the angular momentum $\langle L_z \rangle_2$ [see Eqs. (23) and (33)] at the long-time limit, $t \rightarrow \infty$, are presented. From Eqs. (23), (24), (A8), and (A9) one can conclude that σ_{xx} is given by

$$\begin{aligned} \sigma_{xx} = & \frac{2\gamma \sin(\pi\alpha)}{\pi} \int_0^\infty \frac{r^\alpha}{\tilde{B}(r)} (\hat{M}_1(r) \{ \gamma^2 r^{2\alpha} - r^2 \Omega^2 + (r^2 + \omega_0^2) [r^2 + \omega_0^2 + 2\gamma r^\alpha \cos(\pi\alpha)] \} \\ & + 2\Omega r \hat{M}_3(r) [r^2 + \omega_0^2 + \gamma r^\alpha \cos(\pi\alpha)]) dr + 2\text{Im} \left[\frac{s_1 \hat{M}_3(-s_1)}{C(s_1)} + \frac{s_2 \hat{M}_3(-s_2)}{C(s_2)} \right] - 2\text{Re} \left[\frac{s_1 \hat{M}_1(-s_1)}{C(s_1)} + \frac{s_2 \hat{M}_1(-s_2)}{C(s_2)} \right], \end{aligned} \quad (\text{B1})$$

where

$$\hat{M}_k(s) = Ds^{\delta-1} \hat{H}_{k2}(s), \quad k = 1, 3. \quad (\text{B2})$$

Using formulas (33), (A8), (A9), and (B2) we obtain that the angular momentum $\langle L_z \rangle_2$ can be evaluated as follows:

$$\begin{aligned} \langle L_z \rangle_2 = & \frac{2\gamma \sin(\pi\alpha)}{\pi} \int_0^\infty \frac{r^{\alpha+1}}{\tilde{B}(r)} (\hat{M}_3(r) \{ \gamma^2 r^{2\alpha} - r^2 \Omega^2 + (r^2 + \omega_0^2) [r^2 + \omega_0^2 + 2\gamma r^\alpha \cos(\pi\alpha)] \} \\ & - 2\Omega r \hat{M}_1(r) [r^2 + \omega_0^2 + \gamma r^\alpha \cos(\pi\alpha)]) dr + 2\text{Im} \left[\frac{s_1^2 \hat{M}_1(-s_1)}{C(s_1)} + \frac{s_2^2 \hat{M}_1(-s_2)}{C(s_2)} \right] + 2\text{Re} \left[\frac{s_1^2 \hat{M}_3(-s_1)}{C(s_1)} + \frac{s_2^2 \hat{M}_3(-s_2)}{C(s_2)} \right]. \end{aligned} \quad (\text{B3})$$

In a particular case where the trapping potential is absent ($\omega_0 = 0$), the integral in Eq. (B3) converges only if $\alpha < \frac{2}{3} + \frac{\delta}{3}$. If the memory exponent $\alpha > \frac{2}{3} + \frac{\delta}{3}$, then the mean angular momentum $\langle L_z \rangle_2$ grows unlimited as

$$\langle L_z(t) \rangle_2 \sim t^{3\alpha-\delta-2}, \quad \omega_0 = 0, \quad \alpha > \frac{2}{3} + \frac{\delta}{3}, \quad t \rightarrow \infty. \quad (\text{B4})$$

APPENDIX C: FORMULAS FOR THE CASE OF AN INTERNAL NOISE

In the internal noise situation ($\delta = \alpha$) the variance $\sigma_{xx}(t)$ can be conveniently simplified using Eqs. (3) and (6) and the double Laplace transform technique [51]. From Eqs. (3), (6), (20), (A2), and (A3) we obtain

$$\sigma_{xx}(t) = k_B T \left\{ 2 \int_0^t H_{12}(\tau) d\tau - H_{12}^2(t) - H_{32}^2(t) - \omega_0^2 \left[\int_0^t H_{12}(\tau) d\tau \right]^2 - \omega_0^2 \left[\int_0^t H_{32}(\tau) d\tau \right]^2 \right\}. \quad (\text{C1})$$

In the case of an internal noise, the stationary state corresponds to the equilibrium state. Using Eqs. (A2) and (A3) and the Tauberian theorems [50] the strict $t \rightarrow \infty$ limit in Eq. (C1) gives

$$\sigma_{xx}(\infty) = \frac{k_B T}{\omega_0^2}. \quad (\text{C2})$$

Applying Tauberian theorems in (C1) it can be deduced that the long-time asymptotic behavior of σ_{xx} becomes

$$\sigma_{xx}(t) = \frac{k_B T}{\omega_0^2} \left\{ 1 - \frac{\gamma^2}{\omega_0^4 [\Gamma(1-\alpha)]^2 t^{2\alpha}} + \frac{2\gamma^2 \Omega^2 \alpha (\alpha+3)}{\omega_0^8 [\Gamma(1-\alpha)]^2 t^{2(1+\alpha)}} \right\} + O\left(\frac{1}{t^{3\alpha}}\right), \quad (\text{C3})$$

where $t \gg (\gamma/\omega_0^2)^{1/\alpha}$ and the term proportional to Ω^2 characterizes the main contribution of the magnetic field in the asymptotic expansion (C3). In the case without a trapping potential ($\omega_0 = 0$) the dynamics of the Brownian particle is subdiffusive, the asymptotic behavior of the variance is given by

$$\sigma_{xx}(t) = \frac{2k_B T t^\alpha}{\gamma \Gamma(1+\alpha)} \left[1 - \frac{\Omega^2 \Gamma(1+\alpha)(3\alpha-1)}{\gamma^2 \Gamma(3\alpha) t^{2(1-\alpha)}} \right] + O\left(\frac{1}{t^\lambda}\right), \quad (\text{C4})$$

where $\lambda = 2(1-\alpha)$, if $\alpha < \frac{2}{3}$, and $\lambda = 4-5\alpha$, if $\alpha > \frac{2}{3}$. Here we emphasize that the asymptotic formulas (C3) and (C4) are not applicable close to $\alpha = 1$ (i.e., in the case of a normal diffusion). In this case the relaxation functions $H_{12}(t)$ and $H_{32}(t)$

decay exponentially in time [see also Eqs. (A8) and (A9)], i.e., a slow relaxation of power-law order is absent. Note that the behavior of the normal diffusion process ($\alpha = 1$) of a charged Brownian particle in a constant magnetic field has been theoretically investigated in detail (see, e.g., Refs. [3,46]). Particularly, in the case of $\alpha = 1$ Eq. (C4) reduces to

$$\sigma_{xx}(t) = \frac{2k_B T \gamma t}{\gamma^2 + \Omega^2} + O(1), \quad (\text{C5})$$

which is a result obtained in Ref. [46].

Finally, applying the double Laplace transform technique, from Eqs. (3), (6), (20), (21), (A2), and (A3) it follows that in the case of an internal noise ($\delta = \alpha$) the noise-induced angular momentum $\langle L_z \rangle_2$ [see also Eq. (33)] vanishes for all values of other system parameters, i.e.,

$$\langle L_z \rangle_2 = 0. \quad (\text{C6})$$

-
- [1] C. C. Bloch, *Classical and Quantum Oscillator* (Wiley, New York, 1997).
- [2] S. Chandrasekhar, *Rev. Mod. Phys.* **15**, 1 (1943).
- [3] J. I. Jimenez-Aquino, R. M. Velasco, and F. J. Uribe, *Phys. Rev. E* **77**, 051105 (2008).
- [4] C.-I. Um, K. H. Yeon, and T. F. George, *Phys. Rep.* **362**, 63 (2002).
- [5] M. Turelli, *Theoretical Population Biology* (Academic, New York, 1977).
- [6] N. G. van Kampen, *Stochastic Processes in Physics and Chemistry* (North-Holland, Amsterdam, 1981).
- [7] M. Gitterman, *The Noisy Oscillator: The First Hundred Years, From Einstein Until Now* (World Scientific, Singapore, 2005).
- [8] K. Lindenberg, V. Seshadri, and B. J. West, *Phys. Rev. A* **22**, 2171 (1980).
- [9] R. C. Bourret, U. Frisch, and A. Pouquet, *Physica (Utrecht)* **65**, 303 (1973).
- [10] R. Mankin, K. Laas, T. Laas, and E. Reiter, *Phys. Rev. E* **78**, 031120 (2008).
- [11] R. Benzi, A. Sutera, and A. Vulpiani, *J. Phys. A* **14**, L453 (1981).
- [12] M. Gitterman, *Phys. Rev. E* **67**, 057103 (2003).
- [13] K. Laas, R. Mankin, and A. Rekker, *Phys. Rev. E* **79**, 051128 (2009).
- [14] S. Jiang, F. Guo, Y. Zhou, and T. Gu, *Physica A (Amsterdam)* **375**, 483 (2007).
- [15] S. Burov and E. Barkai, *Phys. Rev. E* **78**, 031112 (2008).
- [16] K. G. Wang and M. Tokuyama, *Physica A (Amsterdam)* **265**, 341 (1999).
- [17] S. C. Kou and X. S. Xie, *Phys. Rev. Lett.* **93**, 180603 (2004).
- [18] E. Soika, R. Mankin, and A. Ainsaar, *Phys. Rev. E* **81**, 011141 (2010).
- [19] W. Götze and M. Sperl, *Phys. Rev. Lett.* **92**, 105701 (2004).
- [20] R. Mankin, K. Laas, and N. Lumi, *Phys. Rev. E* **88**, 042142 (2013).
- [21] R. Mankin, K. Laas, N. Lumi, and A. Rekker, *Phys. Rev. E* **90**, 042127 (2014).
- [22] E. Lutz, *Phys. Rev. E* **64**, 051106 (2001).
- [23] F. Höfling and T. Franosch, *Rep. Prog. Phys.* **76**, 046602 (2013).
- [24] W. Götze and L. Sjögren, *Rep. Prog. Phys.* **55**, 241 (1992).
- [25] T. Carlsson, L. Sjögren, E. Mamontov, and K. Psiuk-Maksymowicz, *Phys. Rev. E* **75**, 031109 (2007).
- [26] S. C. Weber, A. J. Spakowitz, and J. A. Theriot, *Phys. Rev. Lett.* **104**, 238102 (2010).
- [27] Q. Gu, E. A. Schiff, S. Grebner, F. Wang, and R. Schwarz, *Phys. Rev. Lett.* **76**, 3196 (1996).
- [28] I. Goychuk, *Phys. Rev. E* **80**, 046125 (2009).
- [29] I. M. Tolic-Norrelykke, E. L. Munteanu, G. Thon, L. Oddershede, and K. Berg-Sorensen, *Phys. Rev. Lett.* **93**, 078102 (2004).
- [30] R. Granek and J. Klafter, *Phys. Rev. Lett.* **95**, 098106 (2005).
- [31] J. D. Bao and Y. Z. Zhuo, *Phys. Rev. C* **67**, 064606 (2003).
- [32] S. V. Muniandy, W. X. Chew, and C. S. Wong, *Phys. Plasmas* **18**, 013701 (2011).
- [33] Y.-H. Huang and I. Lin, *Phys. Rev. E* **76**, 016403 (2007).
- [34] S. Nunomura, D. Samsonov, S. Zhdanov, and G. Morfill, *Phys. Rev. Lett.* **96**, 015003 (2006).
- [35] H. Asgari, S. V. Muniandy, and C. S. Wong, *Phys. Plasmas* **18**, 083709 (2011).
- [36] I. Holod, A. Zagorodny, and J. Weiland, *Phys. Rev. E* **71**, 046401 (2005).
- [37] J. I. Jimenez-Aquino and M. Romero-Bastida, *Phys. Rev. E* **86**, 061115 (2012).
- [38] J. I. Jimenez-Aquino and M. Romero-Bastida, *Phys. Rev. E* **74**, 041117 (2006).
- [39] L. J. Hou, A. Piel, and P. K. Shukla, *Phys. Rev. Lett.* **102**, 085002 (2009).
- [40] R. Kubo, *Rep. Prog. Phys.* **29**, 255 (1966).
- [41] I. Goychuk, *Adv. Chem. Phys.* **150**, 187 (2012).
- [42] R. Mankin and A. Rekker, *Phys. Rev. E* **81**, 041122 (2010).
- [43] I. Podlubny, *Fractional Differential Equations* (Academic, San Diego, 1999).
- [44] W. Min, G. Luo, B. J. Cherayil, S. C. Kou, and X. S. Xie, *Phys. Rev. Lett.* **94**, 198302 (2005).
- [45] L. Bruno, V. Levi, M. Brunstein, and M. A. Despósito, *Phys. Rev. E* **80**, 011912 (2009).
- [46] B. Kursunoglu, *Ann. Phys.* **17**, 259 (1962).
- [47] A. D. Viñales and M. A. Despósito, *Phys. Rev. E* **75**, 042102 (2007).
- [48] R. Mankin, K. Laas, and A. Sauga, *Phys. Rev. E* **83**, 061131 (2011).
- [49] S. Kempfle, J. Schäfer, and H. Beyer, *Nonlinear Dyn.* **29**, 99 (2002).
- [50] W. Feller, *An Introduction to Probability Theory and its Applications* (Wiley, New York, 1971), Vol. II.
- [51] N. Porttier, *Physica A (Amsterdam)* **317**, 371 (2003).